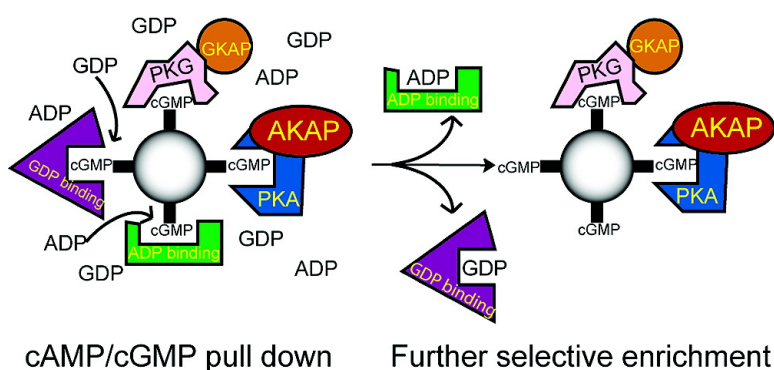


Analysis of the cGMP/cAMP Interactome Using a Chemical Proteomics Approach in Mammalian Heart Tissue Validates Spingosine Kinase Type 1-interacting Protein as a Genuine and Highly Abundant AKAP

Arjen Scholten, Mee Kian Poh, Toon A. B. van Veen, Bas van Breukelen, Marc A. Vos, and Albert J. R. Heck

J. Proteome Res., 2006, 5 (6), 1435-1447 • DOI: 10.1021/pr0600529

Downloaded from <http://pubs.acs.org> on November 17, 2008



More About This Article

Additional resources and features associated with this article are available within the HTML version:

- Supporting Information
- Links to the 2 articles that cite this article, as of the time of this article download
- Access to high resolution figures
- Links to articles and content related to this article
- Copyright permission to reproduce figures and/or text from this article

[View the Full Text HTML](#)

Analysis of the cGMP/cAMP Interactome Using a Chemical Proteomics Approach in Mammalian Heart Tissue Validates Sphingosine Kinase Type 1-interacting Protein as a Genuine and Highly Abundant AKAP

Arjen Scholten,[†] Mee Kian Poh,[†] Toon A. B. van Veen,[‡] Bas van Breukelen,[†] Marc A. Vos,[‡] and Albert J. R. Heck^{*,†}

Department of Biomolecular Mass Spectrometry, Bijvoet Center for Biomolecular Research and Utrecht Institute for Pharmaceutical Sciences, Utrecht University, Sorbonnelaan 16, 3584 CA Utrecht, The Netherlands, and Department of Medical Physiology, Heart Lung Center Utrecht, A. Numan Building, 4th floor, Yalelaan 50, 3584 CM Utrecht, The Netherlands

Received February 20, 2006

The cyclic nucleotide monophosphates cAMP and cGMP play an essential role in many signaling pathways. To analyze which proteins do interact with these second messenger molecules, we developed a chemical proteomics approach using cAMP and cGMP immobilized onto agarose beads, via flexible linkers in the 2- and 8-position of the nucleotide. Optimization of the affinity pull-down procedures in lysates of HEK293 cells revealed that a large variety of proteins could be pulled down specifically. Identification of these proteins by mass spectrometry showed that many of these proteins were indeed genuine cAMP or cGMP binding proteins. However, additionally many of the pulled-down proteins were more abundant AMP/ADP/ATP, GMP/GDP/GTP, or general DNA/RNA binding proteins. Therefore, a sequential elution protocol was developed, eluting proteins from the beads using solutions containing ADP, GDP, cGMP, and/or cAMP, respectively. Using this protocol, we were able to sequentially and selectively elute ADP, GDP, and DNA binding proteins. The fraction left on the beads was further enriched, for cAMP/cGMP binding proteins. Transferring this protocol to the analysis of the cGMP/cAMP "interactome" in rat heart ventricular tissue enabled the specific pull-down of known cAMP/cGMP binding proteins such as cAMP and cGMP dependent protein kinases PKA and PKG, several phosphodiesterases and 6 AKAPs, that interact with PKA. Among the latter class of proteins was the highly abundant sphingosine kinase type1-interacting protein (SKIP), recently proposed to be a potential AKAP. Further bioinformatics analysis endorses that SKIP is indeed a genuine PKA interacting protein, which is highly abundant in heart ventricular tissue.

Keywords: cAMP • cGMP • PKA • PKG • AKAP • chemical proteomics

Introduction

With over 20 000 genes, many splice variants, and post-translational modifications, the cellular proteome is enormously complex.¹ Analyzing tissue even enlarges this complexity, as many different cell types may be present. Presently, one of the major bottlenecks in proteomics is the limited dynamic range in analyzing simultaneously high and low abundant proteins. Therefore, in standard proteomics analyses, low abundant proteins are often missed. To overcome these limitations, sub-proteomic approaches have been introduced, selectively isolating cellular organelles or proteins of particular subclasses. In the latter approach, proteins specifically interacting with a specific bait-protein or antibody may be isolated

from the cellular lysate allowing the analyses of protein complexes and/or signaling pathways.²⁻⁴ Alternatively, small molecules, such as drugs or messenger molecules, can be used as a bait to selectively enrich for proteins that do interact with them, an approach often termed chemical proteomics.⁵⁻⁷

Here, we chose such a chemical proteomics approach to enrich specifically for cGMP and cAMP interacting proteins.⁸ These cyclic nucleotide monophosphate molecules are diffusible intracellular second messenger molecules produced in response to hormone action.⁹ We immobilized cAMP and/or cGMP onto agarose beads, via flexible linkers in either the 2- or 8-position of the nucleotide moiety (Figure 1A).^{10,11}

The principal intracellular target of cAMP is PKA, which is a hetero tetramer that consists of two catalytic subunits that are held in an inactive conformation by a regulatory subunit dimer. However, several other proteins, such as cyclic nucleotide-gated channels, phosphodiesterases, and guanine nucleotide ex-

* To whom correspondence should be addressed. E-mail: a.j.r.heck@chem.uu.nl.

[†] Utrecht University.

[‡] Heart Lung Center Utrecht.

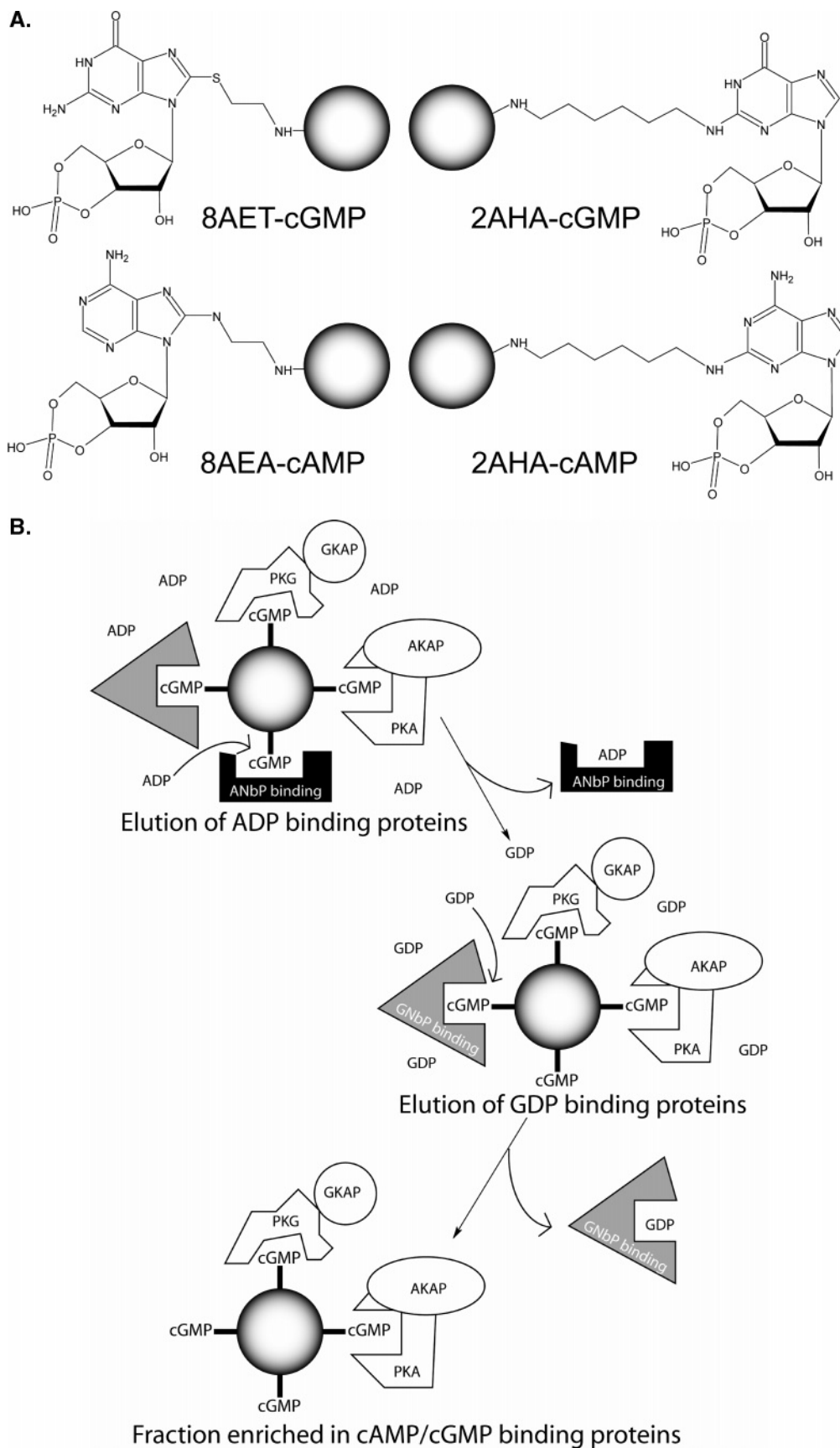


Figure 1. (A) Chemical structures of different immobilized cyclic nucleotides used in this work, (B) Schematic of the sequential elution protocol used for further enrichment of ‘true’ cAMP/cGMP interactors such as PKG and PKA and their binding partners by pre-elution of adenine (ANbP) and guanine (GNbP) nucleotide binding proteins, respectively.

change factors bind to and are activated by cAMP.^{9,12} Additionally, many proteins are thought to bind indirectly to cAMP, for instance through binding with PKA. Compartmentalization of PKA through association with A-kinase anchoring proteins (AKAPs) ensures specificity in signal transduction by tethering the kinase close to its appropriate effectors and substrates.¹³ Most AKAPs bind to the regulatory subunit of PKA and direct the kinase to discrete intracellular locations. Anchored PKA has been shown to be important in various cellular processes, including gene transcription, hormone-mediated insulin secretion and ion-channel modulation. Nowadays, over 70 different AKAPs have been described, which additionally to directing PKA also bring together signal transduction and signal termination molecules in a convergence of signaling pathways.^{9,14,15} PKA's docking domain, close to the N-terminal dimerization domain, forms a tight complex with a conserved 17 amino acid stretch of an AKAP, called the anchoring domain.^{16–18} The sequence and structural organization of the PKA anchoring domain, which forms an amphipathic helix, is the only feature that all AKAPs have in common.

The principal intracellular target of cGMP is PKG; although also for cGMP other binding partners have been described, including phosphodiesterases and cGMP-gated ion channels. The cGMP dependent kinase, PKG, shares homology to PKA,^{19–21} but is involved in very specific signaling pathways such as relaxation of smooth muscle.²² As for PKA, there are two types of PKG, I and II. For both kinases, the type I isozymes are mainly found in the soluble cell fraction, while the type II isoforms are mainly found in the particulate fraction. Compared to PKA, much less well-defined PKG anchoring proteins (GKAPs) have been described.²³ Most notable are the found functional interactions of PKG I α with myosin phosphatase in smooth muscle cells²⁴ and the binding of PKG I β to the IP3-receptor associated protein (IRAG) in tracheal smooth muscle.²⁵

Both cAMP and cGMP signaling are considered important for the functioning of the mammalian heart. In heart tissue, three distinct AKAPs have a strong influence on cation concentration regulation through ion channels: AKAP18 α ,^{26,27} Yotiao²⁸ and mA α KAP.²⁹ Particularly, these three membrane-associated AKAPs have been studied in detail, however, nine others are also known to be present in heart tissue/cardiomyocytes.¹⁵ We assume that even more AKAPs may be present in heart tissue, all most likely with specific functions.

Important for the present study is that PKA and PKG can bind quite tightly to both cAMP and cGMP, and it is believed that each cyclic nucleotide can activate the counterpart kinase,³⁰ although also specific PKA or PKG inhibitors have been described.³¹ Therefore, it may be difficult to selectively pull-down PKA and PKG, and their binding partners using immobilized cyclic nucleotide monophosphate beads.

Here, we describe a comprehensive analysis of proteins that do interact directly or indirectly with cAMP and/or cGMP using cAMP and cGMP immobilized onto agarose beads, via flexible linkers in either the 2- or 8-position (Figure 1A). This revealed that next to genuine cAMP or cGMP binding proteins many more abundant AMP/ADP/ATP, GMP/GDP/GTP, or general DNA/RNA binding proteins were enriched for. To overcome this issue, we continued with the 2-aminoethyl-linked cGMP beads, and introduced a sequential elution protocol, eluting proteins from the beads using solutions containing ADP, GDP, cGMP, and/or cAMP, respectively (Figure 1B). Using this protocol, we were able to elute sequentially and selectively ADP, GDP, cGMP, and cAMP binding proteins. The final elution and

the fraction still remaining on the beads were found to be much more enriched for proteins that do interact directly or indirectly with cAMP or cGMP. Our elution procedure allowed us to enrich for proteins directly binding to the cyclic nucleotides such as PKG and PKA, several phosphodiesterases but also for indirectly binding proteins such as the aforementioned AKAPs. Among the latter class of proteins, enriched from the rat heart ventricular tissue was the highly abundant sphingosine kinase type-1-interacting protein (SKIP), recently proposed to be a potential AKAP. Our approach further validates that SKIP indeed is a genuine PKA interacting protein.

Materials and Methods

Materials. All standard chemicals were purchased from commercial sources and were all of analysis grade, unless stated otherwise. Protease inhibitor cocktail and trypsin were obtained from Roche (Mannheim, Germany). Agarose cyclic nucleotide affinity beads: 8-(2-Aminoethyl)aminoadenosine-3',5'-cyclic monophosphate (8AEA-cAMP), 8-(2-Aminoethyl)thioguanosine-3',5'-cyclic monophosphate (8AET-cGMP), 2'-(6-Aminoethyl)guanosine-3',5'-cyclic monophosphate (2AHA-cAMP) and 2-(6-Aminoethyl)aminoadenosine-3',5'-cyclic monophosphate (2AHAcAMP) were provided by Biolog (Bremen, Germany), see also Figure 1A. The concentration of immobilized cyclic nucleotide on the beads was approximately 6 μ mol/mL, as determined by the manufacturer. HPLC-S gradient grade acetonitrile (AcN) was purchased from Biosolve (Valkenswaard, The Netherlands) and high purity water obtained from a Milli-Q system (Millipore, Bedford, MA) was used for all experiments.

Affinity Pull Down Protocol, HEK293 Cells. HEK293 cells were cultured in suspension in 90% FreeStyle Medium with addition of 10% DMEM, 0.09% fetal calf serum (All Invitrogen, Breda, The Netherlands) and 0.9% primatone (Kerry Biosciences, Tralee, Ireland).

A 50-mL portion of HEK293 cell suspension was harvested at a density of $\sim 1.5 \times 10^6$ cells/mL by centrifugation (30 min, 1000 \times g) and washed once in ice cold PBS before storage at -30 °C. Upon usage, cells were thawed and resuspended in ice-cold lysis buffer (50 mM KPO₄, 150 mM NaCl, 0.1% Tween 20, protease inhibitor cocktail). After daunce homogenization on ice, the lysate was left at 0 °C for another 10 min. Subsequent centrifugation at 20 000 \times g in a tabletop Eppendorf centrifuge (Eppendorf, Hamburg, Germany) at 4 °C yielded separation of soluble and insoluble protein fractions. The soluble fraction (~ 8 mg of total protein) was carefully collected and diluted to protein concentration of 2 mg mL⁻¹ in lysis buffer before addition of the affinity beads (50 μ L dry volume). The lysate-beads suspension was left at 4 °C under agitation for 2 h. Then the beads were washed 6 times in buffer A (50 mM KPO₄, 150 mM NaCl, 0.1% Tween 20) with a total beads to washing volume ratio of 4×10^7 . Next, the beads were boiled in an equal volume of SDS-PAGE loading buffer and subjected to a 12% SDS-PAGE gel.

Elution of Different Nucleotide Binding Fractions. Samples were treated as in the previous experiment, except: before addition of SDS-PAGE loading buffer, the washed beads were subsequently subjected to 50 μ L aliquots of 10 mM ADP, 10 mM GDP, 5 mM cGMP, and 200 mM cAMP in buffer A, for 10 min on ice. To prevent carry-over between the different elutions, beads were washed with 20 volumes of buffer A in between. After elution, beads were treated as before. Eluted samples were treated with 1/5 volume of SDS-page loading buffer and all were subjected to 12% SDS-PAGE electrophoresis.

Rat Heart Tissue. Hearts from 6 months old Wistar rats were excorporated, frozen in liquid nitrogen and stored at -80°C until use. For protein isolation, approximately 150 mg of ventricular tissue was pulverized in a custom-made mortar which was pre-cooled with liquid nitrogen. The powdered tissue was then transferred to 1 mL of ice-cold lysis buffer and left at RT for 5 min. Subsequently, samples were stored on ice for another 10 min and treated as described for the HEK293 cells.

Protein Identification. After gel electrophoresis, gels were subjected to colloidal Coomassie staining or silver staining. For in gel digestion, an adapted protocol of Wilm et al. was used.³² Briefly, complete gel lanes were cut into equally spaced pieces, while in the elution samples, individual protein stained bands were cut out. Gel pieces were subsequently washed with MQ and AcN. Pieces were reduced in DTT and then alkylated with iodoacetamide reagent. After thorough washing, pieces were incubated with trypsin and allowed to digest overnight. Supernatant of the digest was collected and pieces were washed for 30 min in 5% formic acid at RT. Again, supernatant was collected and both were combined.

For HEK293 samples, an Agilent 1100 HPLC system (Agilent Technologies) connected to a Thermo Finnigan LTQ-MS (Thermo Electron, Bremen, Germany) was used. Briefly, peptide extracts (in 10 mM Na_2CO_3 with 2.5% formic acid) were injected on a trap column (Reprosil C18 RP (Dr Maisch, Germany), 20 mm \times 100 μm I.D.) at 5 $\mu\text{L}/\text{min}$ (Subsequently, the peptides were transferred with a split-reduced flow rate of 100 nL/min solvent A (0.1 M acetic acid) on the analytical column (Reprosil C18 RP), 20 cm \times 50 μm I.D.). Elution of the peptides was achieved with a linear gradient from 0 to 40% B (0.1 M acetic acid in 80% (v/v) acetonitrile) in 40 min. The column effluent was directly introduced into the ESI source of the mass spectrometer via a butt-connected nano-ESI emitter (New Objectives, Woburn, MA). The mass spectrometer was operated in the positive ion mode and parent ions were selected for fragmentation in data-dependent mode.

Digested samples from rat ventricular tissue were applied to a nanoscale liquid chromatography tandem mass spectrometry (nano-HPLC-MS/MS) experiment, performed on an Agilent 1100 HPLC system (Agilent Technologies) as described by Meiring et al.³³ When rat ventricular samples were analyzed, the LC-system described above was connected to a 7-Tesla Finnigan LTQ-FT mass spectrometer (Thermo Electron, Bremen, Germany) equipped with a nano electrospray ion source. Briefly, the mass spectrometer was operated in the data dependent mode to automatically switch between MS and MS/MS acquisition. Survey Full scan MS spectra (from m/z 300–1500) were acquired in the FT-ICR with resolution $R = 25\,000$ at m/z 400 (after accumulation to a target value of 5×10^6 in the linear ion trap). The three most intense ions were sequentially isolated for accurate mass measurements by a FT-ICR 'SIM scan' which consisted of 15 Da mass range, $R = 50\,000$ and target accumulation value of $8e^4$. These were then simultaneously fragmented in the linear ion trap using collisionally induced dissociation at a target value of $1e^4$.

After mass spectrometric measurements, data was first analyzed with the MASCOT software (www.matrixscience.com). Then, the MASCOT data was subsequently introduced into the X-Tandem search algorithm of the Scaffold software package (www.proteomesoftware.com). Each search engine has its own strength and weakness. By combining the results of two search engines, one can increase confidence of the peptides that were

found using both engines, as well as gaining extra peptides that are found in either one or the other search engines. Identified proteins were further analyzed for their nucleotide binding properties by using the online SWISS-PROT protein database (www.expasy.org) or by literature searching.

Hidden Markov Searches. To search a heterogeneous sequence database for possible conserved AKAP anchoring domains a motif based hidden Markov model (HMM) was built. For this, sequences of 13 known AKAP proteins were used (ht31, MAP2, TAKAP80, AKAP110, Yotiao, Gravin, AKAP18, AKAP79, DAKAP1, AKAP82, AKAP95, AKAP220, and AKAP-L^{17,34}) with MEME³⁵ to search for conserved motifs with the following constraints; minimum width of motif is 10 nt and maximum width of motif is 18 nt. The motif found with MEME was converted with meta-MEME³⁶ to a motif based HMM. Subsequently, the HMM was used to search fasta databases for the presence of this motif.

Results and Discussion

In this manuscript, we report a method to evaluate cell lysates for cyclic nucleotide binding proteins and their interactors by using affinity beads and specific elutions. Since our method is based on protein precipitation, in the present study, focus is directed to the soluble fraction of the lysates. We evaluated cAMP and cGMP binding proteins, whereby the two different cyclic nucleotides were immobilized on the agarose beads at two different coupling positions, 2' and 8', respectively (Figure 1A).

Different Coupling Positions of the Cyclic Nucleotide Display Different Pull-Down Characteristics. The four different beads were tested using a human embryonic kidney cell line (HEK293). Beads were incubated with a freshly prepared HEK293 lysate, washed thoroughly and applied to 1D-SDS-page (Figure 2). Clearly, the different beads managed to pull down specific protein populations from the lysate (lane 1) Interestingly, different coupling positions resulted into different interactomes as each lane of Figure 2 shows several unique bands. NanoLC-tandem-mass spectrometry (nanoLC-LTQ-MS/MS system) was employed to verify the major proteins that were retrieved by the beads from the lysate. The different beads have several proteins in common: PKA Regulatory subunit I α (PKA I α), PKG type I α (PKG), Heat shock protein 70 kDa (HSP70) and the nucleoside diphosphate kinases (NDPK) A and B (also known as NM23-H1 and H2). The first two cyclic nucleotide dependent kinases were expected as the immobilized baits have these kinases as their primary intracellular targets. As reported before, cGMP beads immobilize PKG and PKA, as do cAMP beads.¹¹ Both HSP70 and NDPK A and B have no cyclic nucleotide binding domain, however, they do have affinity for other nucleotides; HSP70 contains an ATPase domain and therefore binds ATP/ADP.³⁷ The NDPKs are rather unspecific nucleotide binding proteins that interact with different diphosphate nucleotides such as GDP and convert them to triphosphate nucleotides, like GTP.^{38–40} HSP70 and NDPKs are high abundant housekeeping proteins. Other proteins seem to be more specific for a certain type of nucleotide and/or coupling position. For instance, the 8-AEA-cAMP beads (lane 3) efficiently immobilized GAPDH (glyceraldehyde phosphate dehydrogenase) and myosin heavy chain (MHC). GAPDH binds NAD^+ (nicotinamide adenine dinucleotide), which contains an adenine moiety, thereby explaining its affinity for the cAMP-beads. The binding of myosin heavy chain (MHC) to these beads can be explained by binding through its ADP/ATP

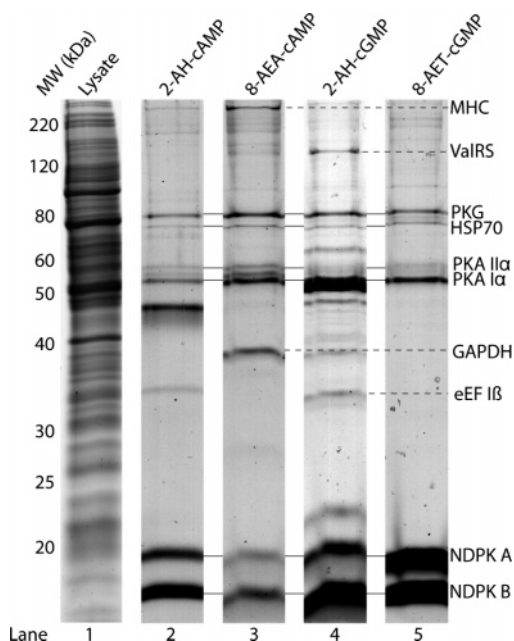


Figure 2. Coomassie stained SDS page gel of HEK293 lysate (lane 1), affinity purified with the four differently immobilized cyclic nucleotide agarose resins. 2AH-cAMP (lane 2), 8AEA-cAMP (lane 3), 2AH-cGMP (lane 4), and 8AET-cGMP (lane 5). Abundant proteins present in the pulled down fractions are depicted next to lane 5, solid lines represent proteins that were found with all four beads, dotted lines indicate proteins predominantly observed in one particular fraction.

domain. The 2-AH-cGMP-beads showed quite a few specific bands in our profiling study (lane 4). Two proteins, valyl-tRNA-synthetase (ValRS), and eukaryotic translation elongation factor 1 β (eEF1 β), were identified in our pull-down and are known to be part of the human eukaryotic translation elongation multiprotein complex 1 (eEF1H).⁴³ In summary, Figure 2 shows that different beads bind different proteins. This is likely caused by the different nature and coupling positions of the ligands. The 2-AH-cGMP-beads seem to bind most specific proteins and were therefore further explored.

Sequential Elution Reveals which Proteins have Affinity for Specific (Cyclic) Nucleotides. Since initial analysis of proteins specifically interacting with 2-AH-cGMP-beads showed a diverse population of proteins, the interactome of these beads was analyzed in-depth by subsequent in-gel digestion and MS analysis of the entire gel lane. Lane 1 in Figure 3 shows that the beads managed to specifically pull down a distinct population of proteins from the HEK293 cell lysate. The use of silver staining revealed more bands in this experiment, compared to the 2AH-cGMP pull down of Figure 2, in which Coomassie staining was applied. Lane 1, Figure 3, was cut into 24 pieces and prepared for MS analysis following in-gel tryptic digestion. Using stringent criteria a total of 42 proteins (H1–H42) were identified with great confidence (shown in the Supporting Information Table 1). Subsequently, the online SWISS-PROT database (www.expasy.org) and literature searching were employed to assess the potential nucleotide binding properties of the identified proteins. Proteins were divided into seven distinct categories: cGMP, cAMP, GMP/GDP/GTP, AMP/ADP/ATP, DNA/RNA, cytoskeletal, and unknown (Supporting Information Table 1 and Figure 3B). This classification is shown in Figure 3B and reveals that only 7% of the identified proteins in the HEK293/2AH-cGMP interactome are cyclic nucleotide

binding proteins. However, many other proteins identified were not just aspecific binding proteins, but are known to have affinity for other forms of adenine and guanine nucleotides such as ADP and GDP and general DNA/RNA binding proteins. Also, the majority of pulled-down proteins (50%) are annotated as cytoskeletal or actin binding proteins. This is likely the cause of the high abundance of cytoplasmic actin (H1) in the pulled down fraction. Since actin is involved in many cytoskeletal structures within the cell, a high abundance of actin/cytoskeletal interacting proteins is not unlikely.

To get more specific information on proteins interacting with cAMP, cGMP (directly or indirectly via the kinases PKA and PKG) a specific elution protocol was designed to reduce the amount of proteins that bind preferentially to other nucleotides. We eluted the beads sequentially with solutions containing ADP, GDP, cGMP, and cAMP. The proteins in the eluted fractions were separated on a 1D gel, displayed in Figure 3a; lane 2 (ADP), lane 3 (GDP), lane 4 (cGMP), and lane 5 (cAMP). Lane 6 displays the proteins that remained still on the beads after this protocol and were eluted by boiling the beads in SDS loading buffer. The elution protocol is based on the expected higher affinity of, for instance, ADP binding proteins for ADP over immobilized 2-AH-cGMP. The first elution performed with 10 mM ADP (lane 2 in Figure 3A) gave rise to several silver stained bands, which were identified, again using the nanoLC–LTQ–MS/MS setup. In complementary experiments, ATP and/or AMP was used instead of ADP, but this led to indistinguishable elution patterns (data not shown). Since ATP activates many proteins, for instance leading to kinase activity, we chose to use ADP. The following proteins were found to elute predominantly in the ADP fraction: Spectrin (H14), α -actinin 4 (H10), HSP70 (H11), cytoplasmic actin (H1) and the NDPK A and B (H2 and H8). H14, H10 and H1 are all part of the cytoskeleton. The finding that HSP70 and actin can be selectively eluted is probably due to the fact that ADP is a higher affinity ligand for these proteins than the immobilized cGMP. Figure 3A shows that NDPK A and B also eluted in other fractions, likely due to the fact that these proteins are quite abundant in the HEK cells and are relatively unspecific in their binding behavior concerning different nucleotides. Strikingly, no significant amount of NDPK eluted with free cGMP, which is also the bait.

In the elution, with 10mM GDP (lane 3), several proteins eluted specifically. Besides the two earlier mentioned constituents of the eEF1H-complex, ValRS (H6) and eEF1 β (H5), we detected now also other known members of this complex, eEF1 α (H4), eEF1 δ (H9), and eEF1 γ (H7).⁴³ It is clear from the comparison of the ADP and GDP elutions (lane 2 and 3, and Figure 3C) that this complex binds preferentially to GDP. In the next elution with 5 mM cGMP (lane 4), we only observed proteins already observed in more abundant quantities in earlier fractions. This was also the case for the cAMP elution (lane 5). Strikingly, PKA and PKG do not elute well from the beads, even when 10 mM cGMP and cAMP solutions were used for the elution. To illustrate this further, in this experiment we used a cAMP-solution of 200 mM, without success. We assume that their affinity for the beads is too high at the current conditions and incubation time, hampering elution with the used concentrations of the cyclic nucleotides at low temperature.⁴⁵ In agreement with this assumption analysis of lane 6, that represents the protein fraction on the beads after the whole elution protocol, yielded the identification of PKG I α (H20) and PKA RI α (H12).

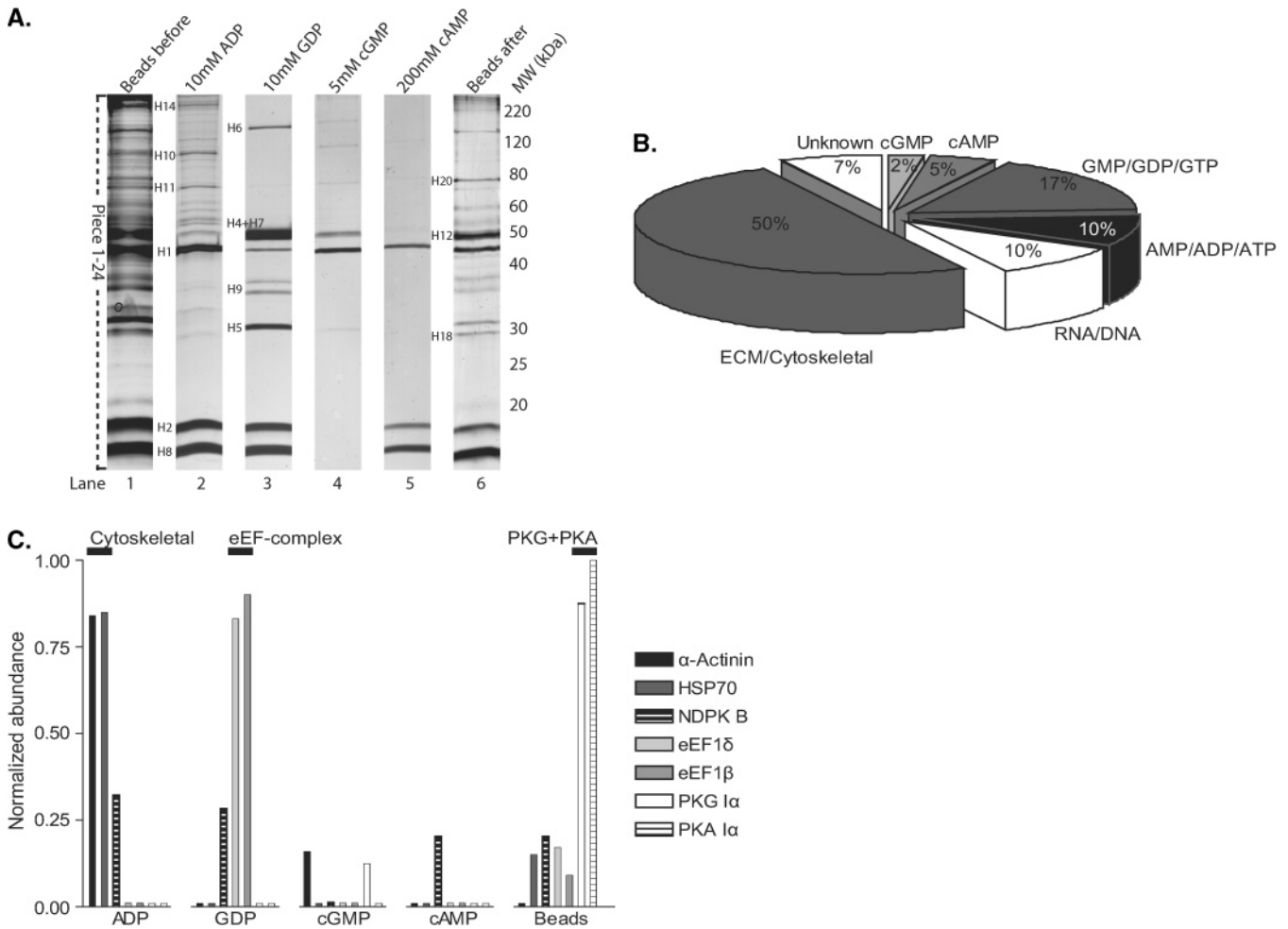


Figure 3. (A) Silver stained SDS page gel of HEK293 lysate treated with 2AH-cGMP beads resulted in a specific pulled down fraction (lane 1) that was sequentially eluted with ADP (lane 2), GDP (lane 3), cGMP (lane 4) and cAMP (lane 5), to yield the PKA/PKG enriched fraction remaining on the beads (lane 6). Abundant proteins annotated in this figure correspond to the identifications reported in the Supporting Information table; H1 Actin cytoplasmic, H2 Nucleoside diphosphate kinase (NDPK) A, H4 Eukaryotic translation elongation factor (eEF) 1 α , H5 eEF1 β , H6 Valyl tRNA synthetase, H7 eEF1 γ , H8 NDPK B, H9 eEF1 δ , H10 α -actinin, H11 Heat shock protein 70kDa, H12 PKA R 1 α , H19 PKG 1 α . (B) Classification of pulled down proteins (lane 1), based on their ligand binding properties. (C) Sequential elution profile of some typical high abundant proteins.

In Figure 3C, we schematically summarize the results of our sequential elution protocol. The relative abundance of several of the abovementioned proteins is given as extracted from the density on the gel after each elution step. This figure clearly illustrates that cytoskeletal proteins such as α -actinin and spectrin, and the housekeeping protein HSP70, can be eluted selectively using ADP. The whole eEF1H-complex was clearly found to elude preferentially in the GDP-fraction. The PKG profile shown in Figure 3c indicates that it is for \sim 90% retained on the beads. Surprisingly, PKA was found to be even better retained on the beads, as no PKA was observed in any of the elution steps. From this experiment, it can be concluded that the cyclic nucleotide interactome is contaminated by abundant proteins that interact with similar ligands such as ADP and GDP. This, together with the high affinity of the beads toward PKG and PKA, makes the sequential elution protocol a perfect tool to further clean up the immobilized fraction.

Analysis of the cGMP/cAMP Interactome in Heart Tissue. With the newly developed elution protocol established, we set out to analyze the cGMP/cAMP interactome in rat ventricular heart tissue using the same 2-AH-cGMP beads and the same experimental protocol described above. The resulting 1D gel

for the affinity pull-down in the rat ventricular heart tissue is shown in Figure 4a. Again, from lane 1 it is evident that 2-AH-cGMP-beads pull a specific protein fraction from the heart lysate that shows both similarities and differences to the one in HEK293 cells. First all proteins immobilized on the beads prior to using the sequential elution procedure were analyzed by cutting lane 1 into 15 gel pieces (B1–B15), as depicted. Because we now used the nanoLC–LTQ–FT–MS/MS system for identification, hundreds of proteins, varying in abundance and thus also in MASCOT scores were identified. We set up a protocol to filter out the background (nonspecific binding proteins) and low abundant proteins. Following analysis of the peptides by LC–LTQ–FT–MS/MS, all individual MASCOT data files were first put into the Scaffold software program (www.proteomesoftware.com). This program then provided a second search algorithm (X-Tandem) that was applied to the data files. Introducing a threshold minimum of 2 unique peptides with a 95% confidence and a total protein identification confidence of 99%, a protein identification dataset of 339 nonredundant proteins was realized. The Scaffold software was also used to exclude keratins and other background proteins, based on the fact that they were found to elute in more than two sections

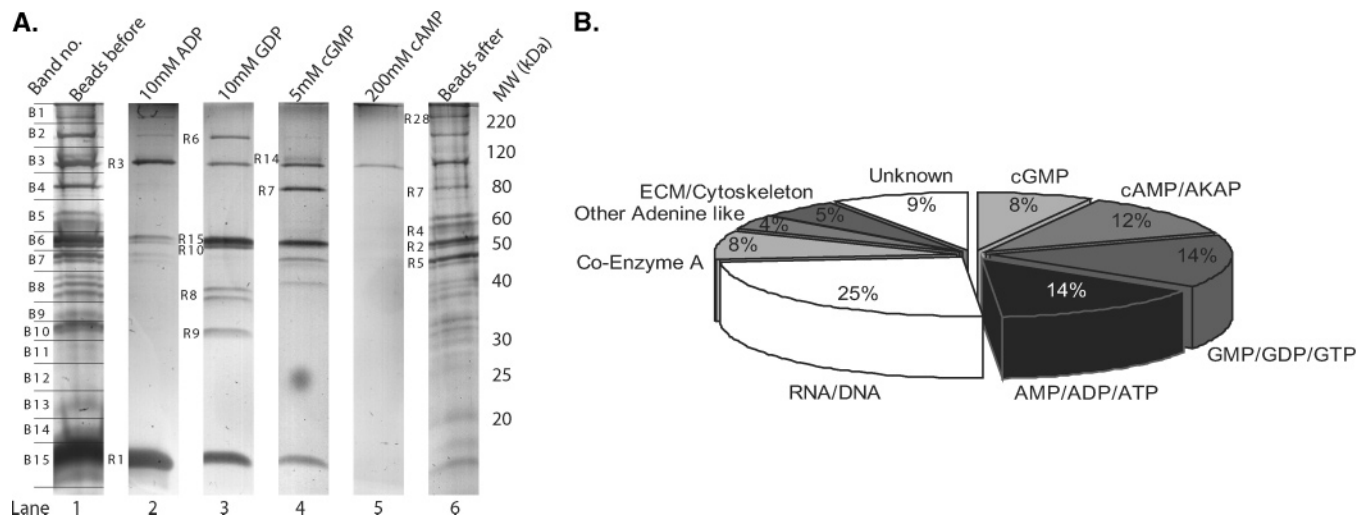


Figure 4. (A) Silver stained SDS-page gel of rat ventricular tissue lysate treated with 2-AH-cGMP beads resulted in a specific pulled down protein fraction (lane 1), that was sequentially eluted with ADP (lane 2), GDP (lane 3), cGMP (lane 4) and cAMP (lane 5), to yield the PKA/PKG enriched fraction remaining on the beads (lane 6). Abundant proteins annotated in this figure correspond to the identification reported in Table 1. (B) Classification of pulled down proteins (lane 1), based on their ligand binding properties.

cut out of the 1D gel, reducing the identification number to 223 proteins. The relative abundance of a protein in our dataset cannot be directly conferred from its protein MASCOT score because it is generally acknowledged that larger proteins yield more peptides resulting in a higher MASCOT score. To gain semiquantitative insight into the relative abundance of the proteins in the data set, we applied a data filtering method, whereby we took into account the amount of unique peptides and the mass of each protein. A variation on a similar approach previously described by others.^{47,48} The procedure was as follows: proteins with a molecular weight of 100kDa or more were required to be present with at least 10 unique peptides, $p < 0.01$, MASCOT score > 34 per peptide. Between 10 and 100 kDa, the minimum amount of unique peptides was set at MW/10 000, with a stringent minimum of 4 peptides for every protein. This means for instance at least 4 peptides for a 20 kDa protein, 5 peptides for a protein between 45 kDa and 54 kDa, and 7 peptides for a protein with a mass around 70 kDa. This stringent filtering procedure enables a better comparison between proteins with a high and a low MW. After applying this filtering method, a list of the most abundant pulled-down rat proteins was realized that contained 76 proteins (R1–R76). These are depicted in Table 1, where these proteins are ordered according to a sequence coverage and abundance factor, calculated by dividing the MW by the amount of MASCOT mass queries ($p < 0.01$). This we assume to be a reasonable measure of relative abundance.^{47,48} In agreement with this procedure we observe that proteins in the top of the list indeed correspond to pronounced bands in lane 3 of the 1D gel; NDPK B (R1) corresponds with the band in gel piece B15, Glycogen phosphorylase (R3), corresponds to the band observed in gel piece B4. The presence of PKA RI (R2) and RII (R4) and PKG (R7) in the top 10 of this list indicates that these proteins are, as expected, well-retained in our protocol and are expressed in the rat heart ventricular tissue.

All annotated protein molecular weights (MWs) seem to correspond with their position on the gel. Exceptions are highlighted in the table. An example is the annotation of eEF1 γ (R10) that was observed in band B6, with an apparent mass of 50 kDa on the gel. In the IPI–RAT database, this protein was annotated with a MW of 72 381 Da (IPI00470317), however, no

eEF1 γ was observed in band B4 around 70 kDa. In the SWISS-PROT database, the correct mass of 49 930 (Q68FR6) has been assigned to this gene in agreement with the position on the 1D gel.³⁷ The SWISS-PROT annotation lacks the N-terminal 210 amino acids from the IPI–RAT database annotated gene. In addition, none of the peptides matched to eEF1 γ were present in this N-terminal part, strongly suggesting that the currently annotated mass in the IPI–RAT database is incorrect. Again, all proteins in the dataset were annotated for their possible nucleotide and/or DNA binding preferences as described above. These data are also depicted in Table 1 and in Figure 4B.

Comparison of the cAMP/cGMP Interactome in Rat Ventricular Heart Tissue and HEK293 Cells. The presence of PKG (R7) and PKA (R2, R4) in the rat ventricular heart tissue was immediately confirmed from our data. For PKG we only observed the α -isoform, as in the HEK293 cells. The regulatory domain of PKA was as expected present in two different isoforms; α and $\text{II}\alpha$, since these two isoforms are reported to be most abundant in the mammalian heart.⁴⁹ Besides PKG and PKA, several other proteins were observed in both HEK293 cells and rat ventricular tissue. The eEF1H complex (R6, R8, R9, R10, and R15) was pulled-down in the heart tissue, consisting of the same subunits, and again eluting preferentially in the GDP fraction. In the heart tissue, we also detected another aminoacyl-tRNA synthase, cysteinyl-tRNA synthase (CysRS) (R45), a homologue of ValRS.⁵⁰ NDPK B (R1) was detected, however, NDPK A not. Another isoform of a NDPK could be identified as NDPK3 or DR-NM23 (R16).

Interestingly, our pull-down approach seemed less “hindered” by abundant cytoskeletal proteins in the rat heart tissue when compared to the mammalian HEK293 cells. High abundant HEK293 protein cytoplasmic actin (H1) (or β -actin) is absent in the rat ventricular dataset, as are many of the other in HEK293 pulled-down cytoskeletal proteins. It is possible that actin present in heart tissue is much more constrained in the highly ordered cytoskeletal network of cardiac muscle. These forms of actin are less likely to be present in the soluble protein fraction, and consequently also less in our pull down experiment.

Abundant proteins in the rat heart tissue data set not observed in the HEK293 data set, are isoforms of glycogen

Table 1. Identified Proteins of 2AH-cGMP Pull Down in Rat Ventricular Tissue, Ordered According to MW/Amount of MASCOT Queries

no.	protein	SWISS acc. no.	IPI rat. acc. no.	binds	Mw	no. of queries	unique peptides	MASCOT score	band no.	Mw/queries
R1	Nucleoside diphosphate kinase B	P22392	IPI00188610	GDP/GTP/GMP	17254	102	13	792	15	169.2
R2	cAMP-dependent protein kinase type RI α	P10644	IPI00654466	AKAP/cAMP	42919	122	31	1940	6	351.8
R3	Glycogen phosphorylase, muscle form	P11217	IPI00190181	ADP/ATP/AMP	97063	163	60	3516	3	595.5
R4	cAMP-dependent protein kinase type RI α	P13861	IPI00365600	AKAP/cAMP	45494	74	30	1871	5	614.8
R5	Glutaryl-Coenzyme A dehydrogenase	Q92947	IPI00476550	CoA	49265	63	30	1630	7	782.0
R6	Valyl-tRNA synthetase	P26640	IPI00372557	eEF complex	141169	145	61	3739	2	973.6
R7	cGMP dependent kinase type I α	Q13976	IPI00361251	cGMP	68256	70	30	1692	4	975.1
R8	Eukaryotic translation elongation factor 1 δ	Q96138	IPI00199740	eEF complex	72207 ^b	66	23	1557	8	1094.1
R9	Eukaryotic translation elongation factor 1 β	P24534	IPI00557435	eEF complex	24642	22	10	639	10	1120.1
R10	Eukaryotic translation elongation factor 1 γ	Q68FR6	IPI00470317	eEF complex	72381 ^b	60	25	1446	7	1206.3
R11	Decorin precursor (Bone proteoglycan II)	P07585	IPI00199861	ECM	39762 ^b	31	18	1024	3	1282.6
R12	Acyl-CoA dehydrogenase, long-chain	P28330	IPI00211225	CoA	47824	35	19	1304	7	1366.4
R13	Cpo protein, Coproporphyrinogen III oxidase.	P36551	IPI00191745	Other/Unknown	93774 ^b	57	28	1677	8	1645.2
R14	cGMP-dependent 3',5'-cyclic phosphodiesterase type 2A	O00408	IPI00199076	cGMP	104579	50	32	2155	3	2091.6
R15	Eukaryotic translation elongation factor 1 α	Q05639	IPI00568311	GDP/GTP/GMP	50404	24	16	875	5	2100.2
R16	Nucleoside diphosphate kinase DR-nm23	Q13232	IPI00198988	GDP/GTP/GMP	19059	9	6	350	14	2117.7
R17	LOC500183 protein	Q7Z473	IPI00388002	Other/Unknown	25658	12	6	414	11	2138.1
R18	Glycogen phosphorylase, brain isoform	P11216	IPI00357945	ADP/ATP/AMP	96659	41	18	1566	3	2357.5
R19	Polymerase I-transcript release factor	Q6NZI2	IPI00201300	RNA	43864	18	14	888	5	2436.9
R20	Alpha Crystallin B chain heat shock protein beta 5	P02511	IPI00215465	ADP etc via HSP	20058	8	5	304	13	2507.3
R21	Transcription factor A, mitochondrial precursor (HMG protein)	Q00059	IPI00327334	RNA/DNA	28151	11	9	404	12	2559.2
R22	Histone H1.2	P16403	IPI00231650	RNA/DNA	21825	8	7	490	10	2728.1
R23	ANP32B (PHAPI2/APRIL)	Q92688	IPI00564251	RNA/DNA	31024	11	6	428	9	2820.4
R24	Heat Shock Protein 70 kDa	P38646	IPI00363265	ADP/ATP/AMP	73780	26	21	1405	4	2837.7
R25	Nuclease sensitive element binding protein 1	P67809	IPI00551815	RNA/DNA	35691	12	10	619	6	2974.2
R26	Heterogeneous nuclear ribonucleoprotein M	P52272	IPI00209148	RNA	74283	24	22	1153	4	3095.1
R27	Acyl-CoA dehydrogenase family member 8	Q94KU7	IPI00360664	CoA	28069	9	6	338	8	3118.8
R28	Sphingosine kinase type 1-interacting protein (181kDa protein)	Q6NSW3 ^d	IPI00362975	AKAP	181171	57	45	2983	1	3178.4
R29	Triosephosphate isomerase	P60174	IPI00231767	Other/Unknown	26755	8	7	386	11	3344.3
R30	Transcription factor Pur-beta	Q96QR8	IPI00189358	RNA/DNA	33494	10	9	482	8	3349.4
R31	Ca/calmodulin-dependent 3',5'-cyclic nucleotide phosphodiesterase 1A	P54750	IPI00189442	cGMP	61806	18	14	901	5	3433.7
R32	Hypoxanthine-guanine phosphoribosyltransferase	P00492	IPI00464890	GDP/GTP/GMP	24444	7	5	330	11	3491.9
R33	UBF2 of Nucleolar transcription factor 1	P17480	IPI00566459	RNA	84897	23	21	1020	3	3691.2
R34	Pyridoxal kinase	O00764	IPI00372837	Other Adenine like	34868	9	7	443	9	3874.2
R35	Death associated protein 3	P51398	IPI00564895	GTP/GDP/GMP	44448	11	10	665	8	4040.7
R36	Nucleophosmin	P06748	IPI00382264	RNA	32522	8	8	427	8	4065.2
R37	Mitogen-activated protein kinase 1, Erk	P28482	IPI00562552	ADP/ATP/AMP	41231	10	9	507	7	4123.1
R38	Cysteine and glycine-rich protein 3	P50461	IPI00198497	ECM/Cytoskeleton	20771	5	4	225	14	4154.2
R39	Lupus La protein homolog	P05455	IPI00471902	RNA	47730	11	11	656	7	4339.1
R40	Glypican-1 precursor (Heparan sulfate proteoglycan core protein)	P35052	IPI00194930	ECM	61677	14	10	623	1	4405.5
R41	Igj_predicted protein	P01591	IPI00363901	Other/Unknown	17755	4	4	230	12	4438.7
R42	Dehydrogenase/reductase, SDR family member 6	Q9BUT1	IPI00201136	Other Adenine like	27642	6	6	387	13	4607.0
R43	Trifunctional enzyme beta subunit	P55084	IPI00198467	CoA	51364	11	10	539	7	4669.4
R44	Glycogen synthase kinase-3 β	P49841	IPI00569456	AKAP binding protein	46695	10	8	431	7	4669.5
R45	Cysteinyl-tRNA Synthetase	P49589	IPI00563516	eEF complex	94801	19	18	1001	3	4989.5
R46	A-Kinase anchor protein 2 (AKAP-KL)	Q9Y2D5	IPI00390678	AKAP	96046	19	16	971	2	5055.0
R47	Nucleosome assembly protein 1-like 4 (NAP2)	Q99733	IPI00327185	RNA/DNA	47256	9	9	490	6	5250.7
R48	Myosin light polypeptide 3	P08590	IPI00231788	ADP via Myosin	21993	4	4	235	12	5498.3
R49	Nucleolin	P19338	IPI00198884	RNA	77212	14	13	682	4	5515.2
R50	Immunoglobulin (LOC314521 protein)	Q96EY0	IPI00560817	Other/Unknown	68300	12	9	527	4	5691.7
R51	Hypothetical protein (hnRNP-Dlike)	na	IPI00363719	RNA	35254	6	6	282	8	5875.7
R52	Ca/calmodulin-dependent 3',5'-cyclic nucleotide phosphodiesterase 1C	Q14123	IPI00198173	cGMP PDE	71870	12	8	572	4	5989.1
R53	Guanylate binding protein 1, interferon-inducible	P32455	IPI00363520	GDP/GTP/GMP	90848	15	12	617	4	6056.6
R54	cGMP-specific 3',5'-cyclic phosphodiesterase type 5A	O76074	IPI00328073	cGMP	94478	15	13	808	3	6298.5
R55	Predicted similar to RIKEN cDNA 2810422B04	Q96EY7	IPI00204675	Other/Unknown	66230	10	7	449	4	6623.0
R56	3-ketoacyl-CoA thiolase	P42765	IPI00201413	CoA	41827	6	6	363	7	6971.1
R57	Homologue of zebrafish ES1	P30042	IPI00191783	RNA/DNA	28137	4	4	183	11	7034.2
R58	U2 small nuclear ribonucleoprotein polypeptide A	P09661	IPI00192279	RNA/DNA	28282	4	4	178	10	7070.5
R59	Tubulin β 2	P07437	IPI00400573	Other/Unknown	49751	7	7	348	5	7107.3
R60	Acyl-CoA dehydrogenase, very-long-chain	P49748	IPI00213057	CoA	71227	10	9	599	5	7122.7

Table 1. (Continued)

no.	protein	SWISS acc. no.	IPI rat. acc. no.	binds	Mw	no. of queries	unique peptides	MASCOT score	band no.	Mw/queries
R61	Glyceraldehyde-3-phosphate dehydrogenase	P00354	IPI00561110	Other Adenine like	35664	5	5	324	8	7132.8
R62	J domain of DnaJ-like-protein 1	Q8WXX5	IPI00215575	ADP via R24	29942	4	4	196	9	7485.6
R63	Ca/calmodulin-dependent 3',5'-cyclic nucleotide phosphodiesterase 1B	Q01064	IPI00199077	cGMP PDE	61203	8	6	355	5	7650.4
R64	Heterogeneous nuclear ribonucleoprotein R	O43390	IPI00564342	RNA	70812	9	6	346	4	7868.0
R65	A-kinase anchor protein 7 (AKAP18 gamma/delta isoform)	O43687	IPI00421609	AKAP	39375	5	5	253	7	7875.1
R66	hnRNP U (SP120)	Q00839	IPI00210090	RNA	87676	11	11	559	3	7970.5
R67	32 kDa protein (hnRNP2/B1)	Q99729	IPI00212969	RNA	32431	4	4	193	8	8107.6
R68	ATP synthase, H ⁺ transporting, gamma polypeptide 1	Q5VYP3	IPI00396906	ADP/ATP/AMP	32957	4	4	195	10	8239.3
R69	Perlecan (heparan sulfate proteoglycan 2)	P98160	IPI00388323	ECM	505873	61	54	3183	1	8293.0
R70	A-Kinase anchor protein 10 (D-AKAP2)	O43572	IPI00471827	AKAP	75351	9	8	389	4	8372.3
R71	Glycogen branching enzyme	Q04446	IPI00560733	ADP via R3	58815	7	7	450	4	8402.1
R72	Tripartite motif protein 26	Q99PN3 ^a	IPI00422036	RNA/DNA	62574	7	7	330	5	8939.1
R73	A-kinase anchor protein 1 (D-AKAP1)	Q92667	IPI00231915	AKAP	91672	9	9	509	3	10185.8
R74	A-kinase anchor protein 11 (AKAP220)	Q94KA4	IPI00607183	AKAP	228165	17	14	797	2	13421.5
R75	Myosin heavy chain, cardiac muscle α -isoform	P13533	IPI00476111	ADP/ATP/AMP	223352	16	16	934	1	13959.5
R76	Glycogen Debranching Enzyme	P35573	IPI00373422	ADP via R3	174202	12	12	591	2	14516.8

^a SWISS-PROT accession numbers from human, as no available in rat. ^b Molecular weights in bold are masses that contradict with the mass observed by the position on the gel.

phosphorylase (R3, R18) and a large range of Coenzyme-A (CoA) binding proteins (e.g., R5, R12, and R27). CoA also contains an adenine moiety, explaining its presence in our dataset. The phosphorylases are very important for energy supply to the cardiac muscle by regulating the glucose-to-glycogen ratio of the cell.

The significance of cAMP and cGMP signaling in ventricular tissue, is reiterated, not only by the presence of PKA and PKG, but by a much higher diversity of cyclic nucleotide binding proteins and their known binding partners. Besides PKG several cGMP binding phosphodiesterases (PDEs) were detected (R14, R31, R52, R54, and R63), among which was the cGMP stimulated PDE5 (R54), the target of sildenafil in the treatment of erectile dysfunction. Most interestingly, several indirect binding proteins were also detected, among them several PKA anchoring proteins; AKAPs (e.g., R46, R65).

cGMP Interacting Proteins. Besides the expected cGMP binding kinase PKG (R7), a distinct other group of cGMP regulated proteins was detected, the phosphodiesterases (PDEs). Three members of the PDE family were identified: PDE1 (R31, R52, and R63), PDE2 (R14), and PDE5 (R54). PDEs are the endpoint of cyclic nucleotide signaling as these proteins degrade cAMP to AMP and cGMP to GMP. PDEs form an intriguing group of proteins that intersect between the cAMP and cGMP pathway. Some PDEs are selective in the degradation of cAMP (e.g., PDE4), others are selective for cGMP (e.g., PDE5), while several do not significantly distinguish between cAMP or cGMP (e.g., PDE1, PDE2).⁵¹ The most abundant PDE in our pull down is PDE2. All three known human splice isoforms of PDE2 originate from a single gene.⁵² This PDE is selectively activated by cGMP, but hydrolyzes both cAMP and cGMP. cGMP stimulation takes place through binding of it to the N-terminal regulatory domain, also annotated as a GAF domain. It is therefore likely that PDE2 interacts with our cGMP-beads through the GAF-domain of the PDE. PDE2 was reported to be expressed in rat, bovine and human cardiac tissue, consistent with its presence in our pull down.⁵² The three splice forms of PDE2 differ at the N-terminal domain. However from the limited number of PDE2 peptides we sequenced with MS, we could not unambiguously determine which splice variants were present. PDE1 is known to exist in three distinct isoforms

in most mammals, 1A, 1B, and 1C.⁵¹ Previously, it has been shown that mRNA of 1B⁵³ and 1C⁵⁴ is present in cardiac myocytes. Here we confirm that all three PDE1 isoforms are present in heart tissue, as specific peptides for each isoform were identified (data not shown). The third observed PDE family member is PDE5. This cGMP stimulated, cGMP-selective PDE is mainly found in lung,⁵⁵ platelets and vascular smooth muscle, but our data clearly reveal the presence of PDE5 also in rat ventricular tissue. PDE5 contains two GAF-domains in its N-terminus that strongly regulate its activity. An additional feedback mechanism is imposed by PKG that phosphorylates PDE5 at the first GAF-domain, making it more susceptible for cGMP stimulation.⁵⁶

The fact we did not observe any of the described membrane incorporated cGMP-gated ion channels is likely due to the absence of these particulate proteins in our soluble lysate fraction or their potential low expression levels in heart.

cAMP Interacting Proteins. Besides the expected two types of cAMP dependent kinase, PKA (I α , R2 I α , R4), a distinct other group of proteins was detected in our pull down, the PKA anchoring proteins, or AKAPs. Fink *et al.*⁵⁷ showed the high importance of PKA-AKAP binding in the function of the heart. Most AKAPs tether PKA RII, although also dual specificity AKAPs (D-AKAPs) and RI specific AKAPs have been identified.⁹ PKA RII, and to a lesser extent, RI are highly spatially regulated by their binding to different AKAPs, which in their own right can act as scaffolds for binding other proteins as well. To date, as far as we know, 12 AKAPs have been identified in heart tissue: AKAP1 (D-AKAP1), AKAP5 (AKAP79), AKAP6 (mAKAP), AKAP7 (AKAP18), AKAP8 (AKAP95), AKAP9 (yotiao), AKAP10 (D-AKAP2), AKAP11 (AKAP220), AKAP12 (gravin), AKAP13 (AKAP-Lbc, Ht31), BIG2, and ezrin.¹⁵

In our experiments, four AKAPs earlier described as being expressed in cardiac cells or tissue were detected; AKAP1 (R73), AKAP7 (R65), AKAP10 (R70), and AKAP11 (R74). An AKAP not previously reported to be expressed in heart was also identified; AKAP2 (R46), also known as AKAP-KL.⁵⁸ Possibly most interesting is the identification and relative high abundance of SKIP (R28) (Sphingosine Kinase Interacting Protein 1) in our pull down. In mouse, SKIP was earlier described to have sequence

homology to AKAP 11. Our data ascertain SKIP to be a real and abundant AKAP in rat ventricular tissue, detected with about 50 peptides.

New AKAP in Heart and Elucidation of Splice Variants of Several AKAPs. On the basis of the amount of unique peptides, the PKA RII binding AKAP2 (AKAP-KL, R46) seems to be an abundant soluble AKAP in rat heart tissue. Previously, AKAP2 has been assigned as an actin cytoskeletal binding AKAP, with a very specific tissue distribution in the particulate fractions of mouse lung, thymus, cerebellum and kidney.⁵⁸ In kidney, AKAP2 was only observed in the nonsoluble, particulate fractions of the tissue lysate. Interestingly, Dong et al. did not find AKAP2 in the particulate fraction of mouse heart by western blotting.⁵⁸ In contrast, we find AKAP2 to be a relatively high abundant protein in the soluble fraction of rat ventricular tissue.

By analyzing the MS data in more detail, we could distinguish the presence of several specific splice isoforms of certain AKAPs. For AKAP7, the position on the gel around 40 kDa determined that the heavy splice variants γ , and/or δ are present in our data set.⁵⁹ For AKAP1, we could determine the presence of splice isoform 1c.^{60,61} Interesting for AKAP11 was the presence of a binding partner, other than PKA, in our data; glycogen synthase kinase-3 β (GSK3 β)⁶²

SKIP, Sphingosine Kinase Interacting Protein 1 is a Genuine AKAP. SKIP, or sphingosine kinase interacting protein 1 (R28), was recently identified by yeast-2-hybrid screening as an anchoring protein for sphingosine kinase 1 (SPHK1) in mouse.⁷² According to Northern blot analysis, expression of SKIP was highest in heart, but it was also found to be present in spleen, ovary, and brain.⁷² When analyzing the MS spectra of SKIP peptides by MASCOT in combination with the IPI-Rat database, two protein annotations for SKIP were suggested. The first annotated as 181 kDa protein (IPI00476739, SKIP-L(ong)), the second as Predicted: similar to SKIP (IPI00362975) with a calculated mass of 151 kDa (SKIP-S(hort)). Both sequences were aligned using ClustalW and it became clear that the sequence of SKIP-L was extended at both N- and C-terminus (amino acids (aa) 1–115 and 1464–1653, respectively) compared to SKIP-S (Figure 5A). Interestingly, both sequences had unique sequence stretches in the part between aa 115–1464. SKIP-S had a 20 aa stretch inserted between position 609 and 610 of SKIP-L. SKIP-L's amino acids 228–230 were absent in SKIP-S. In the MS data, both shared 39 unique peptides, also depicted in Figure 5A. In addition, we discovered 6 peptides to be unique for the SKIP-L and 3 peptides encompassing the 20 amino acid stretch unique for SKIP-S (Figure 5A). These data pointed toward the presence of two SKIP splice forms in rat heart, or a redundant false annotation of either protein in the IPI-Rat database. In the nonredundant SWISS-PROT database, only mouse SKIP (mSKIP) is annotated (Q6NSW3, 181 kDa, Figure 5A). This sequence was highly identical to SKIP-L, as it contained 228–230 and lacked the 20 amino acid stretch from SKIP-S. When the human isoform (hSKIP), obtained by BLAST analysis of SKIP-L was also aligned, we observed that hSKIP contained both unique sequences. These data could indicate the presence of two isoforms, or could indicate that the hSKIP sequence is the only accurate sequence of a SKIP protein. Since no SKIP specific high affinity antibody is available yet for Western blotting, we could not resolve this issue.

It was also reported previously that the C-terminal domain (aa 1107–1656) of mSKIP shares 35–40% identity to AKAP11

in mouse.⁷² BLAST analysis of the C-terminal domain of SKIP-L (aa 1505–1637) revealed it to be homologue to the rat isoform of AKAP11 (gi|62661753), with 32% identity and 53% similarity.

Although SKIP shows a partly similar sequence to AKAP11, no association of PKA with SKIP has been described. Since in our experiments SKIP, and AKAP11, co-purify with PKA, and are also retained on the 2-AH-cGMP beads after the elution protocol, we now provide evidence that SKIP is a true AKAP. The presence of SKIP in the soluble fraction of the heart ventricular lysate is in close agreement with confocal microscopy experiments performed by Lacaná et al., who observed SKIP to be mainly cytosolic and nuclear excluded in NIH 3T3 fibroblast cells, despite the presence of suspected nuclear localization sequences.⁷² To really define SKIP as an AKAP, the amphipathic helix that comprises the anchoring domain has to be present. We applied a bioinformatics tool to localize this domain; a motif based hidden Markov model (HMM).^{35,36} When constructing the motif from 13 different known AKAP anchoring sequences³⁴, one motif was found (Figure 5B), encompassing 18 amino acids with an information content of 27.1 bits and an E-value of 4.6×10^{-16} . Depicted is the obtained sequence logo, in which the size of the letters represents the importance of a specific amino acid at a certain position. Previously, the importance of hydrophobic residues at position 6, 9, 10, 14, and 17 was established,^{34,73} which is also illustrated by our model in which all of these positions are hydrophobic. The obtained consensus sequence that was constructed for the HMM-motif was as follows: TLEEYANRLVQNVIQMAV. Representation of this motif in a helical wheel (Figure 5D, left wheel) shows that all hydrophobic residues are present on one side of the helix while charged residues were mainly found on the other side, making it an amphipathic helix model sequence. To increase the confidence that our model could indeed predict AKAP sequences, we constructed a fasta database of 1000 random protein sequences and spiked it with several different AKAP sequences. All AKAP sequences in this database were matched to the HMM-motif, whereas the others were not, confirming the validity of the obtained model (data not shown). When the HMM-motif was applied to a fasta database containing SKIP-L, SKIP-S, mSKIP, and hSKIP, a conserved amino acid stretch that bears high similarity to the other anchoring sequences was discovered (Figure 5A and C). We strongly suggest that this sequence represents SKIP's amphipathic helix that anchors PKA. This is further illustrated by the helical wheel representation of SKIP-L 909–923 in Figure 5D, that also shows a hydrophobic and a hydrophilic side, that is required for interaction with PKA's docking domain, as described earlier.¹⁶ The presence of SKIP in our pull down experiment, together with its co-purification in the PKA fraction, remaining on the beads after the different elution steps and the presence of a conserved anchoring domain, classifies SKIP as a true AKAP. Further studies should elucidate SKIP's function in heart, where we show it to be highly expressed.

Possible Role for SKIP. The observed high abundance of SKIP in our pull-down hints at a potential specific function for this sphingosine kinase and PKA interacting protein in heart tissue. On the basis of the currently available literature it is tempting to speculate on a possible role of SKIP as a converging scaffold of both cAMP and sphingosine signaling.

Sphingosine kinase type 1 (SPHK1) mediates the levels of two sphingolipids; sphingosine and sphingosine-1-phosphate (S1P). SPHK1 phosphorylates sphingosine to form S1P. The former has pro-apoptotic properties, while the latter shows

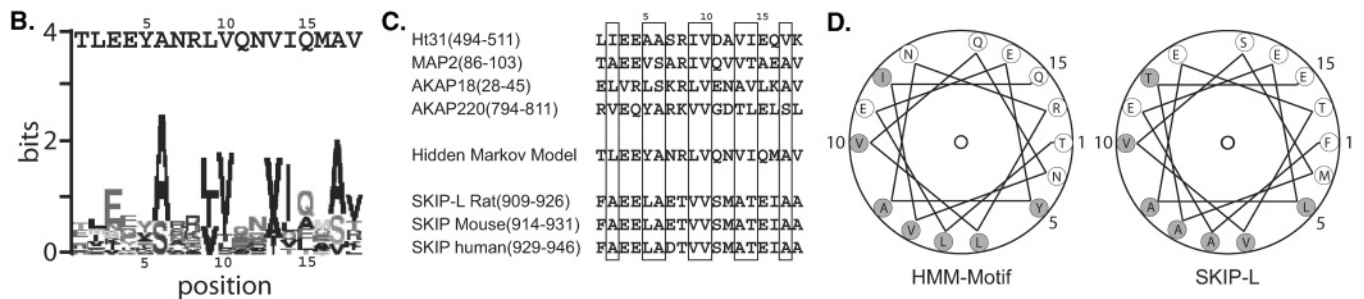


Figure 5. (A) Sequence alignment of 4 different SKIP isoforms. Also depicted are all peptides observed by mass spectrometry that could be matched to both SKIP rat isoforms in the IPI-Rat database (solid lines), or matched uniquely to SKIP-L (long dashed lines) or SKIP-S (short dashed lines). The proposed amphipathic anchoring helix is boxed. (B) Sequence logo of the 18 amino acid hidden Markov model (HMM) AKAP motif. In this representation, larger amino acid codes represent higher conservation of this particular amino acid at a certain position. Depicted on top is the resulting HMM sequence, representing the optimized AKAP consensus motif. (C) Alignment of the anchoring domains (amphipathic helices) of AKAPs Hi31, MAP2, AKAP18, and AKAP220 with our HMM model consensus sequence and the proposed anchoring sequences of SKIP. Conserved hydrophobic residues, essential for interaction with PKA, are boxed. (D) Helical wheel representation of the HMM model consensus sequence and the proposed amphipathic helix of SKIP. Hydrophobic residues are depicted in gray.

anti-apoptotic behavior. Therefore it is believed that the balance between these two sphingolipids, which is mediated by SPHK1, is a strong determinant of cell fate. Not surprising, SPHK1 is implicated to be an oncogene as overexpression of SPHK1 results likely in increased levels of S1P, which in turn promotes cell survival and protects cells from apoptotic insults.⁷⁴

Furthermore, it has recently been established that cAMP-induced differentiation of human leukemia cells (HL60) to granulocytes goes through the MEK/ERK pathway and that this is mediated by increased SPHK1 activity.⁷⁵ Also, increased expression of SKIP reduces SPHK1 activity, indicating that SKIP might function as a SPHK1 activity switch.⁷² We show that SKIP is an AKAP and since AKAPs seem to mediate almost any form of cAMP/PKA signaling, it does not seem unlikely that SKIP would be mediating cAMP induced activation of SPHK1, or sphingosine induced activation of PKA. In agreement with the latter hypothesis, Ma et al. showed that phosphorylation of the multifunctional adaptor protein 14-3-3 ζ by PKA is initiated by sphingosine, but not by cAMP.⁷⁶ 14-3-3 family proteins are phosphoserine-binding proteins that interact with and modulate the functions of many key cellular proteins involved in proliferation, cell survival and cell cycle control.⁷⁷ These considerations make the finding of Erk (R37) in our pull down experiment potentially interesting, as it may hint toward complex formation of important cell differentiating factors on SKIP, including the three kinases ERK, PKA and SPHK1. All of these results indicate that SKIP may act as a converging scaffold of both cAMP and sphingosine signaling, although more functional studies should be undertaken to validate this hypothesis.

Conclusion

We developed a comprehensive chemical proteomics approach that may be used to efficiently enrich cGMP and cAMP binding proteins, and their possible binding partners, from complex cellular lysates and heart tissue. By using a sequential elution protocol, further specific enrichment could be achieved as cross-interacting nucleotide binding proteins could be pre-eluted by utilizing their higher affinity for their natural ligands, such as ADP and GDP. Applying this approach to the analysis of the cGMP/cAMP “interactome” in rat heart ventricular tissue enabled the specific pull-down of known cAMP/cGMP binding proteins such as cAMP and cGMP dependent protein kinases PKA and PKG, several phosphodiesterases and six AKAPs, that interact with PKA. Most of these AKAPs were described earlier to be present in cytosolic extracts. Among the latter class of proteins was the highly abundant, so far only theoretically suggested AKAP, sphingosine kinase type1-interacting protein (SKIP). Our data, backed up by bioinformatics analysis endorses that SKIP is indeed a genuine PKA interacting protein. We suggest that SKIP may act as a converging scaffold linking cAMP and sphingosine signaling pathways.

Acknowledgment. The authors would like to thank Wiegner Hemrika, Roland Romijn, and Niels Kaldenhoven from the ABC expression facility at Utrecht University for providing the HEK293 cells. Martijn Pinkse and Shabaz Mohammed are acknowledged for support with the FT–MS analysis. This study is financially supported by The Netherlands Organization for Scientific Research (NWO, Grant No. 916.36.012, TvV) and The Netherlands Proteomics Centre (www.netherlandsproteomicscenter.nl).

Supporting Information Available: Supporting Information Table; 42 proteins (H1–H42) identified with high confidence in the 2AH–cGMP pull down in HEK293 cells. This material is available free of charge via the Internet at <http://pubs.acs.org>.

References

- (1) Aebersold, R.; Mann, M. *Nature* **2003**, *422*, 198–207.
- (2) Bouwmeester, T.; Bauch, A.; Ruffner, H.; Angrand, P. O.; Bergamini, G.; Coughton, K.; Cruciat, C.; Eberhard, D.; Gagneur, J.; Ghidelli, S.; Hopf, C.; Huhse, B.; Mangano, R.; Michon, A. M.; Schirle, M.; Schlegl, J.; Schwab, M.; Stein, M. A.; Bauer, A.; Casari, G.; Drewes, G.; Gavin, A. C.; Jackson, D. B.; Joberty, G.; Neubauer, G.; Rick, J.; Kuster, B.; Superti-Furga, G. *Nat. Cell. Biol.* **2004**, *6*, 97–105.
- (3) Gavin, A. C.; Bosche, M.; Krause, R.; Grandi, P.; Marzioch, M.; Bauer, A.; Schultz, J.; Rick, J. M.; Michon, A. M.; Cruciat, C. M.; Remor, M.; Hofert, C.; Schelder, M.; Brajenovic, M.; Ruffner, H.; Merino, A.; Klein, K.; Hudak, M.; Dickson, D.; Rudi, T.; Gnau, V.; Bauch, A.; Bastuck, S.; Huhse, B.; Leutwein, C.; Heurtier, M. A.; Copley, R. R.; Edelmann, A.; Querfurth, E.; Rybin, V.; Drewes, G.; Raida, M.; Bouwmeester, T.; Bork, P.; Seraphin, B.; Kuster, B.; Neubauer, G.; Superti-Furga, G. *Nature* **2002**, *415*, 141–147.
- (4) Blagojev, B.; Kratchmarova, I.; Ong, S. E.; Nielsen, M.; Foster, L. J.; Mann, M. *Nat. Biotechnol.* **2003**, *21*, 315–318.
- (5) Oda, Y.; Owa, T.; Sato, T.; Boucher, B.; Daniels, S.; Yamanaka, H.; Shinohara, Y.; Yokoi, A.; Kuromitsu, J.; Nagasu, T. *Anal. Chem.* **2003**, *75*, 2159–2165.
- (6) Speers, A. E.; Cravatt, B. F. *Chembiochem.* **2004**, *5*, 41–47.
- (7) Daub, H.; Godl, K.; Brehmer, D.; Klebl, B.; Muller, G. *Assay Drug Dev. Technol.* **2004**, *2*, 215–224.
- (8) Dremier, S.; Kopperud, R.; Doskeland, S. O.; Dumont, J. E.; Maenhaut, C. *FEBS Lett.* **2003**, *546*, 103–107.
- (9) Wong, W.; Scott, J. D. *Nat. Rev. Mol. Cell. Biol.* **2004**, *5*, 959–970.
- (10) Laukens, K.; Roef, L.; Witters, E.; Slegers, H.; Van Onckelen, H. *FEBS Lett.* **2001**, *508*, 75–79.
- (11) Kim, E.; Park, J. M. *J. Biochem. Mol. Biol.* **2003**, *36*, 299–304.
- (12) Bos, J. L. *Nat. Rev. Mol. Cell. Biol.* **2003**, *4*, 733–738.
- (13) Colledge, M.; Scott, J. D. *Trends Cell Biol.* **1999**, *9*, 216–221.
- (14) Langeberg, L. K.; Scott, J. D. *J. Cell Sci.* **2005**, *118*, 3217–3220.
- (15) Ruehr, M. L.; Russell, M. A.; Bond, M. J. *Mol. Cell. Cardiol.* **2004**, *37*, 653–665.
- (16) Carr, D. W.; Stofko-Hahn, R. E.; Fraser, I. D.; Bishop, S. M.; Acott, T. S.; Brennan, R. G.; Scott, J. D. *J. Biol. Chem.* **1991**, *266*, 14188–14192.
- (17) Newlon, M. G.; Roy, M.; Morikis, D.; Hausken, Z. E.; Coghlan, V.; Scott, J. D.; Jennings, P. A. *Nat. Struct. Biol.* **1999**, *6*, 222–227.
- (18) Herberg, F. W.; Maleszka, A.; Eide, T.; Vossebein, L.; Tasken, K. J. *Mol. Biol.* **2000**, *298*, 329–339.
- (19) Scott, J. D. *Pharmacol. Ther.* **1991**, *50*, 123–145.
- (20) Francis, S. H.; Poteet-Smith, C.; Busch, J. L.; Richie-Jannetta, R.; Corbin, J. D. *Front Biosci.* **2002**, *7*, d580–592.
- (21) Pfeifer, A.; Ruth, P.; Dostmann, W.; Sausbier, M.; Klatt, P.; Hofmann, F. *Rev. Physiol. Biochem. Pharmacol.* **1999**, *135*, 105–149.
- (22) Lincoln, T. M.; Dey, N.; Sellak, H. *J. Appl. Physiol.* **2001**, *91*, 1421–1430.
- (23) Vo, N. K.; Gettemy, J. M.; Coghlan, V. M. *Biochem. Biophys. Res. Commun.* **1998**, *246*, 831–835.
- (24) Surks, H. K.; Mochizuki, N.; Kasai, Y.; Georgescu, S. P.; Tang, K. M.; Ito, M.; Lincoln, T. M.; Mendelsohn, M. E. *Science* **1999**, *286*, 1583–1587.
- (25) Schlossmann, J.; Ammendola, A.; Ashman, K.; Zong, X.; Huber, A.; Neubauer, G.; Wang, G. X.; Allescher, H. D.; Korth, M.; Wilm, M.; Hofmann, F.; Ruth, P. *Nature* **2000**, *404*, 197–201.
- (26) Fraser, I. D.; Tavalin, S. J.; Lester, L. B.; Langeberg, L. K.; Westphal, A. M.; Dean, R. A.; Marrion, N. V.; Scott, J. D. *Embo J.* **1998**, *17*, 2261–2272.
- (27) Gray, P. C.; Johnson, B. D.; Westenbroek, R. E.; Hays, L. G.; Yates, J. R., 3rd; Scheuer, T.; Catterall, W. A.; Murphy, B. J. *Neuron* **1998**, *20*, 1017–1026.
- (28) Marx, S. O.; Kurokawa, J.; Reiken, S.; Motoike, H.; D’Armiento, J.; Marks, A. R.; Kass, R. S. *Science* **2002**, *295*, 496–499.
- (29) Kapiloff, M. S.; Schillace, R. V.; Westphal, A. M.; Scott, J. D. *J. Cell Sci.* **1999**, *112* (Pt 16), 2725–2736.
- (30) Pelligrino, D. A.; Wang, Q. *Prog. Neurobiol.* **1998**, *56*, 1–18.
- (31) Dostmann, W. R.; Taylor, M. S.; Nickl, C. K.; Brayden, J. E.; Frank, R.; Tegge, W. J. *Proc. Natl. Acad. Sci. U.S.A.* **2000**, *97*, 14772–14777.

- (32) Wilm, M.; Shevchenko, A.; Houthaevae, T.; Breit, S.; Schweigerer, L.; Fotsis, T.; Mann, M. *Nature* **1996**, *379*, 466–469.
- (33) Meiring, H. D.; van der Heeft, E.; ten Hove, G. J.; de Jong, A. P. J. *M. J. Sep. Sci.* **2002**, *25*, 557–568.
- (34) Newlon, M. G.; Roy, M.; Morikis, D.; Carr, D. W.; Westphal, R.; Scott, J. D.; Jennings, P. A. *Embo J.* **2001**, *20*, 1651–1662.
- (35) Bailey, T. L.; Elkan, C. In *Proceedings of the Second International Conference on Intelligence Systems for Biology*; AAAI Press: Menlo Park, California, 1994; pp 28–36.
- (36) Grundy, W. N.; Bailey, T. L.; Elkan, C. P.; Baker, M. E. *Comput. Appl. Biosci.* **1997**, *13*, 397–406.
- (37) www.expasy.org.
- (38) Lecroisey, A.; Lascu, I.; Bominaar, A.; Veron, M.; Delepiepierre, M. *Biochemistry* **1995**, *34*, 12445–12450.
- (39) Gonin, P.; Xu, Y.; Milon, L.; Dabernat, S.; Morr, M.; Kumar, R.; Lacombe, M. L.; Janin, J.; Lascu, I. *Biochemistry* **1999**, *38*, 7265–7272.
- (40) Cervoni, L.; Lascu, I.; Xu, Y.; Gonin, P.; Morr, M.; Merouani, M.; Janin, J.; Giartosio, A. *Biochemistry* **2001**, *40*, 4583–4589.
- (41) Lombardi, D.; Lacombe, M. L.; Paggi, M. G. *J. Cell. Physiol.* **2000**, *182*, 144–149.
- (42) Niitsu, N.; Okabe-Kado, J.; Okamoto, M.; Takagi, T.; Yoshida, T.; Aoki, S.; Hirano, M.; Honma, Y. *Blood* **2001**, *97*, 1202–1210.
- (43) Mansilla, F.; Friis, I.; Jadidi, M.; Nielsen, K. M.; Clark, B. F.; Knudsen, C. R. *Biochem. J.* **2002**, *365*, 669–676.
- (44) Bec, G.; Kerjan, P.; Waller, J. P. *J. Biol. Chem.* **1994**, *269*, 2086–2092.
- (45) Døskeland, S. O.; Ogreid, D. *J. Biol. Chem.* **1984**, *259*, 2291–2301.
- (46) Mackay, F.; Ambrose, C. *Cytokine Growth Factor Rev.* **2003**, *14*, 311–324.
- (47) Sanders, S. L.; Jennings, J.; Canutescu, A.; Link, A. J.; Weil, P. A. *Mol. Cell. Biol.* **2002**, *22*, 4723–4738.
- (48) Ishihama, Y.; Oda, Y.; Tabata, T.; Sato, T.; Nagasu, T.; Rappsilber, J.; Mann, M. *Mol. Cell. Proteomics* **2005**, *4*, 1265–1272.
- (49) Krall, J.; Tasken, K.; Staheli, J.; Jahnsen, T.; Movsesian, M. A. *J. Mol. Cell. Cardiol.* **1999**, *31*, 971–980.
- (50) Kim, J. E.; Kim, K. H.; Lee, S. W.; Seol, W.; Shiba, K.; Kim, S. *Nucleic Acids Res.* **2000**, *28*, 2866–2872.
- (51) Maurice, D. H.; Palmer, D.; Tilley, D. G.; Dunkerley, H. A.; Netherton, S. J.; Raymond, D. R.; Elbatarny, H. S.; Jimmo, S. L. *Mol. Pharmacol.* **2003**, *64*, 533–546.
- (52) Rosman, G. J.; Martins, T. J.; Sonnenburg, W. K.; Beavo, J. A.; Ferguson, K.; Loughney, K. *Gene* **1997**, *191*, 89–95.
- (53) Yu, J.; Wolda, S. L.; Frazier, A. L.; Florio, V. A.; Martins, T. J.; Snyder, P. B.; Harris, E. A.; McCaw, K. N.; Farrell, C. A.; Steiner, B.; Bentley, J. K.; Beavo, J. A.; Ferguson, K.; Gelinas, R. *Cell Signal* **1997**, *9*, 519–529.
- (54) Verde, I.; Vandecasteele, G.; Lezoualc'h, F.; Fischmeister, R. *Br. J. Pharmacol.* **1999**, *127*, 65–74.
- (55) Corbin, J. D.; Beasley, A.; Blount, M. A.; Francis, S. H. *Biochem. Biophys. Res. Commun.* **2005**, *334*, 930–938.
- (56) Rybalkin, S. D.; Rybalkina, I. G.; Shimizu-Albergine, M.; Tang, X. B.; Beavo, J. A. *Embo J.* **2003**, *22*, 469–478.
- (57) Fink, M. A.; Zakhary, D. R.; Mackey, J. A.; Desnoyer, R. W.; Apperson-Hansen, C.; Damron, D. S.; Bond, M. *Circ. Res.* **2001**, *88*, 291–297.
- (58) Dong, F.; Feldmesser, M.; Casadevall, A.; Rubin, C. S. *J. Biol. Chem.* **1998**, *273*, 6533–6541.
- (59) Henn, V.; Edemir, B.; Stefan, E.; Wiesner, B.; Lorenz, D.; Theilig, F.; Schmitt, R.; Vossebein, L.; Tamma, G.; Beyermann, M.; Krause, E.; Herberg, F. W.; Valenti, G.; Bachmann, S.; Rosenthal, W.; Klussmann, E. *J. Biol. Chem.* **2004**, *279*, 26654–26665.
- (60) Huang, L. J.; Wang, L.; Ma, Y.; Durick, K.; Perkins, G.; Deerinck, T. J.; Ellisman, M. H.; Taylor, S. S. *J. Cell Biol.* **1999**, *145*, 951–959.
- (61) Ma, Y.; Taylor, S. *J. Biol. Chem.* **2002**, *277*, 27328–27336.
- (62) Tanji, C.; Yamamoto, H.; Yorioka, N.; Kohno, N.; Kikuchi, K.; Kikuchi, A. *J. Biol. Chem.* **2002**, *277*, 36955–36961.
- (63) Brown, R. L.; August, S. L.; Williams, C. J.; Moss, S. B. *Biochem. Biophys. Res. Commun.* **2003**, *306*, 394–401.
- (64) Lin, R. Y.; Moss, S. B.; Rubin, C. S. *J. Biol. Chem.* **1995**, *270*, 27804.
- (65) Huang, L. J.; Durick, K.; Weiner, J. A.; Chun, J.; Taylor, S. S. *J. Biol. Chem.* **1997**, *272*, 8057–8064.
- (66) Huang, L. J.; Durick, K.; Weiner, J. A.; Chun, J.; Taylor, S. S. *Proc. Natl. Acad. Sci. U.S.A.* **1997**, *94*, 11184–11189.
- (67) Wang, L.; Sunahara, R. K.; Krumins, A.; Perkins, G.; Crochiere, M. L.; Mackey, M.; Bell, S.; Ellisman, M. H.; Taylor, S. S. *Proc. Natl. Acad. Sci. U.S.A.* **2001**, *98*, 3220–3225.
- (68) Perkins, G. A.; Wang, L.; Huang, L. J.; Humphries, K.; Yao, V. J.; Martone, M.; Deerinck, T. J.; Barraclough, D. M.; Violin, J. D.; Smith, D.; Newton, A.; Scott, J. D.; Taylor, S. S.; Ellisman, M. H. *BMC Neurosci.* **2001**, *2*, 17.
- (69) Lester, L. B.; Coghlan, V. M.; Nauert, B.; Scott, J. D. *J. Biol. Chem.* **1996**, *271*, 9460–9465.
- (70) Reinton, N.; Collas, P.; Haugen, T. B.; Skälhegg, B. S.; Hansson, V.; Jahnsen, T.; Tasken, K. *Dev. Biol.* **2000**, *223*, 194–204.
- (71) Schillace, R. V.; Scott, J. D. *Curr. Biol.* **1999**, *9*, 321–324.
- (72) Lacana, E.; Maceyka, M.; Milstien, S.; Spiegel, S. *J. Biol. Chem.* **2002**, *277*, 32947–32953.
- (73) Alto, N. M.; Soderling, S. H.; Hoshi, N.; Langeberg, L. K.; Fayos, R.; Jennings, P. A.; Scott, J. D. *Proc. Natl. Acad. Sci. U.S.A.* **2003**, *100*, 4445–4450.
- (74) Olivera, A.; Kohama, T.; Edsall, L.; Nava, V.; Cuvillier, O.; Poulton, S.; Spiegel, S. *J. Cell. Biol.* **1999**, *147*, 545–558.
- (75) Koda, M.; Murate, T.; Wang, S.; Ohguchi, K.; Sobue, S.; Ikeda, M.; Tamiya-Koizumi, K.; Igarashi, Y.; Nozawa, Y.; Banno, Y. *Biochim. Biophys. Acta* **2005**, *1733*, 101–110.
- (76) Ma, Y.; Pitson, S.; Hercus, T.; Murphy, J.; Lopez, A.; Woodcock, J. *J. Biol. Chem.* **2005**, *280*, 26011–26017.
- (77) Fu, H.; Subramanian, R. R.; Masters, S. C. *Annu. Rev. Pharmacol. Toxicol.* **2000**, *40*, 617–647.

PR0600529